

Understanding Ability of 3D Integral Displays to Provide Accurate Out-of-focus Retinal Blur

Ginni Grover, Oscar Nestares, Ronald Azuma; Intel Corporation; Santa Clara, California, USA

Abstract

Many current far-eye 3D displays are incapable of providing accurate out-of-focus blur on the retina and hence cause discomfort with prolonged use. This out-of-focus blur rendered on the retina is an important stimulus for the accommodation response of the eye and hence is one of the major depth cues. Properly designed integral displays can render this out-of-focus blur accurately.

In this paper, we report a rigorous simulation study of far-eye integral displays to study their ability to render depth and the out-of-focus blur on the retina. The beam propagation simulation includes the effects of diffraction from light propagation through the free space, the apertures of lenslet and the eye pupil, to calculate spot sizes on the retina formed by multiple views entering the eye. Upon comparing them with the spot sizes from the real objects and taking into account depth of field and spatial resolution of the eye, we determine the minimum number of views needed in the pupil for accurate retinal blur. In other words, we determine the minimum pixel pitch needed for the screen of a given integral display configuration. We do this for integral displays with varying pixel sizes, lenslet parameters and viewing distances to confirm our results.

One of the key results of the study is that roughly 10 views are needed in a 4 mm pupil to generate out-of-focus blur similar to the real world. The 10 views are along one dimension only and out-of-focus-blur is only analyzed for the fovea. We also note that about 20 views in a 4 mm pupil in one dimension in the pupil would be more than sufficient for accurate out-of-focus blur on the fovea. Although 2-3 views in the pupil may start triggering accommodation response as shown previously, much higher density of views is needed to mimic the real world blur.

Introduction

Integral displays (ID) are a form of light field displays which are promising candidates for true 3D displays as they can provide consistent depth cues for 3D perception. They have been studied for more than a century now, starting from the initial work in 1908 [1]. They have been especially well studied theoretically and experimentally in last three decades to understand their capability as true 3D displays [2]. Different configurations of near-eye [3-4] and far-eye [5] 3D displays based on IDs have been presented. Among far-eye 3D displays, they present a big advantage over other methods as they can be seen with a naked eye and by multiple viewers simultaneously.

IDs are clearly understood as promising candidates for far-eye 3D displays as they can theoretically provide all the depth cues consistently for 3D perception in humans. We prove that unlike many current 3D displays they are capable of providing accurate out-of-focus blur on the retina which is an important stimulus for the accommodation response of the eye. Retinal blur is a major depth cue contributing to our 3D perception and generating an accommodation response of the eye [6]. It was previously shown

that at least two views are needed to enter the eye to generate the accommodation response [7]. Another study for light field displays has been reported which conducted a rigorous analysis for optimal number of views [8]; however, we found that the specific case of far-eye integral displays we show here is not covered by that analysis. Thus, a rigorous study of how different number of views affect the accuracy of the rendered out-of-focus blur has not been reported for far-eye integral displays, with screen-lens spacing equal to focal length. It is important to understand retinal blur for these displays as it affects how closely these IDs can mimic the real world.

In this paper, we determine how many views are required to generate accurate retinal blur, similar to the real world. In the first section, we provide the image formation model in the IDs we study, discussing how multiple views entering the eye contribute to the determination of depth and blur. In the second section, we discuss the beam propagation simulation method used to simulate light from IDs and real world objects. Thirdly, we show results comparing IDs with varying pixel pitches (or number of views) against the real world objects to determine the optimal number of views. In the fourth section, we provide a summary of various results for IDs, which to our knowledge have not been reported previously.

Image Formation Model

Out of the several configurations possible for IDs [9], we only study the case when the spacing between the screen and the lenslets is equal to the focal length of the lenslets. A schematic of this configuration is shown in Fig. 1. The lens pitch (p) and the pixel pitch (p_d) of the screen determine important characteristics of the IDs, namely, depth of field (dof), spatial resolution (r) and eyebox width (w) [9]. As shown in ref. [9], reducing the pixel pitch of the screen improves these characteristics and sends more views in the eyebox. Thus, it is well understood that smaller pixel pitch is preferred. However, none of the previous results, including the characteristic equation, help to understand what is an ideal number of views in the eye's pupil to match the real world.

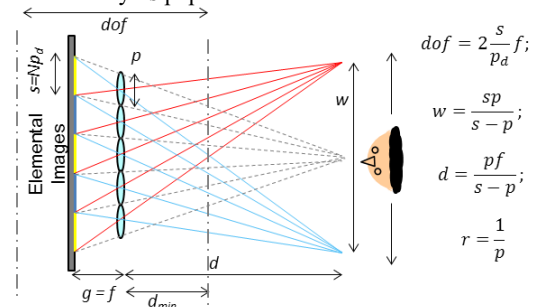


Figure 1: Far-eye Integral display configuration used here, where spacing between screen and the lenslet is equal to the focal length of the lenslet, $g = f$.

Using the ID model where spacing is equal to the lens focal length (i.e., $g=f$), Fig. 2 shows how rays from two lenses intersect to create points at different depths and then enter the eye's pupil. Due to finite size of the lenslet and screen pixel, only a few angles per depth point are incident on the pupil. Whereas, a continuous range of angles enter the eye's pupil for a real world object point. Also seen is the fact that depth points very close to the lens – in front and behind – have only a single ray angle (view) entering the eye. We show this quantitatively in the results section.

In the ID configuration we have analyzed, the discrete nature of screen pixels and lenslets renders a large number of discrete depth planes or points. Although the actual depth planes rendered will depend on the scene, the number of possible depth planes which are possible for an ID is fixed. Similarly, the locations of these possible depth planes is fixed, determined by the geometrical parameters of the screen, lenslet array and eye position. Fig. 2 (bottom) shows a schematic of an ID with maximum 5 views, all of which enter the eye's pupil. Six consecutively placed lenslets of the ID are shown and chief rays from each pixel to the eye pupil are traced. Note the figure is not to scale. But it depicts that any point where rays from two different lenslets intersect is a possible depth point. If needed, we can determine the location of all these possible depth planes mathematically from the geometry. However, this number is very large and therefore it is not feasible to study all the possible depth planes. To make the problem tractable we limit our study to depth points formed by two adjacent lenslets, one of which is centered at the eye. By analyzing these two lenslets we get a reasonable range of depth points to study the formation of in-focus and out-of-focus retinal images of these depth points. We also restrict the study to depth points formed by the intersection of the on-axis pixel of the central lens with all the pixels from the adjacent lens, as shown in Fig. 2 (top left). Lens 1 can refer to the lens where the eye is centered on the ID. Figure 3 shows how the in-focus and out-of-focus images of different depth points are formed on the retina, when multiple views or angles enter the eye's pupil.

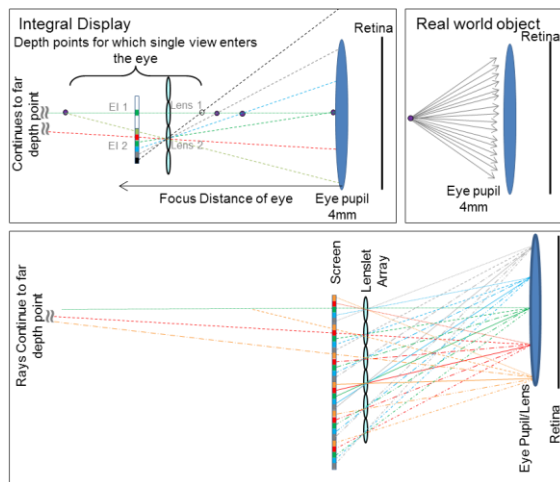


Figure 2: Schematics of IDs to understand formation of depth points. Top Left: rays from two adjacent lenslets in an ID. Rays from the Lens 2 intersect the on-axis ray from Lens 1 to give different depth points. In an ID, for each depth point, only discrete ray angles are possible. Top Right: A real world object which has continuous angles entering the eye. Bottom: schematic of an ID with maximum 5 views, all of which enter the eye's pupil. Please note that the schematics are not to scale.

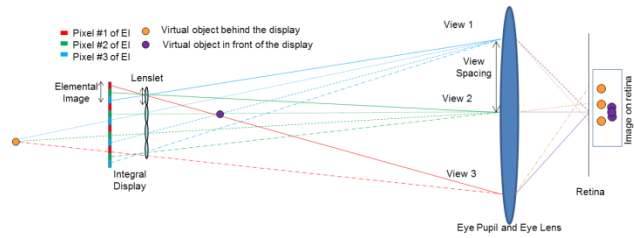


Figure 3: Formation of in-focus (purple point) and out-of-focus (orange point) depth points on the retina when viewing an ID.

Simulation Details

As mentioned in the previous section, we are just analyzing two adjacent lenslets in the IDs for studying formation of in-focus and out-of-focus depth blurs. We simulate light from two adjacent lenslets using the Fast Fourier transform beam propagation method (FFTBPM) [10]. In the beam propagation simulation, we assume thin paraxial optics with finite aperture for the lenslets and the eye. The simulation includes diffraction effects from free-space propagation, lenslet aperture and eye pupil aperture. In the simulation, we have not included effect of light emitting from the screen pixel and propagation to the lenslet. Instead, we assume that pixel is an infinitesimally small point source emitting light uniformly in all directions. The diverging light emitted by the pixel is incident on and clipped by the lenslet, which then converts it to a collimated beam of finite width (equal to the lenslet aperture). This collimated beam diffracts as it propagates to the viewer's eye. The simulation and the analysis are done in 1D and results can be directly extrapolated to 2D. Simulation of light propagation from two adjacent lenslets and spot sizes formed on the pupil and retina are shown in Fig.4.

We model the real world object as an infinitesimally small point source emitting light uniformly in all directions. This diverging uniform wavefront is then incident on the eye pupil/lens. So, for a given depth point, we apply an incident diverging wavefront (depending on the object depth) on the converging eye lens. The focal power of the eye lens depends on the focus position of the eye. We then do FFTBPM till the retina [11]. The FFTBPM simulation is done at 5x higher resolution than the retina pixel size. For visualization of some results the pixel size of the fovea of the eye is assumed to be $2.5 \mu\text{m}$. We assume the eye pupil diameter to be 2-6 mm in the simulations but only show results for 4 mm pupil size.

Results

From the FFTBPM simulation, we obtain the spots on the retina for light emitting at different angles from the lenslet. Only a single on-axis emission angle is simulated for the lenslet centered on the optical axis of the eye, Lens 1. A range of emission angles are simulated for the adjacent lenslet, Lens 2. The emission angle geometrically relates to the pixel position on the screen under the lens. Also, Fig. 2 shows how different emission angles from Lens 2 intersect with the on-axis ray from Lens 1 to give different depth points. In the simulation, the focal position of the eye is also varied to analyze the blur. We discuss and visualize various results as follows.

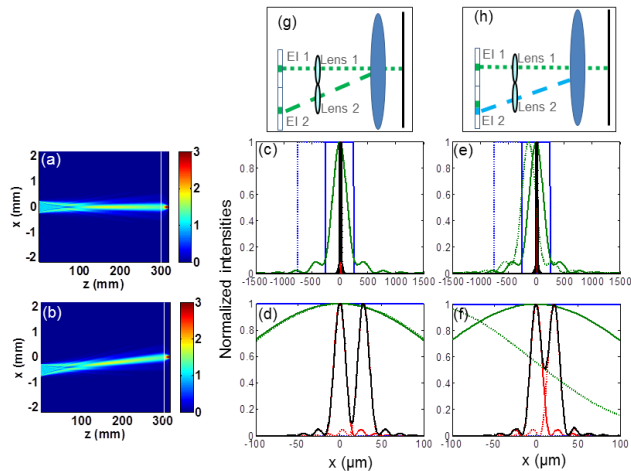


Figure 4: (a-b) FFTBPM simulation for a collimated light beam emitting from a lenslet (small aperture on the left edge of the image), propagating 300 mm in free space to the eye's lens (at the plane marked with a vertical white line), to the retina on the right edge of the image. (c-f) Plots showing light intensities at the lenslet, the pupil and retina planes. The curves from the on-axis Lens 1 are solid and adjacent Lens 2 are dashed. Light intensity emitting from the lenslet is shown in blue, intensity at the eye's pupil plane in green and individual retinal focal spots in red. Light from two different lenslets is spatially incoherent and added at the retina plane (black). (d) and (f) are zoomed in plots of (c) and (e), respectively. (c-d) show the case when light from two lenslets creates the same view, as shown in sketch (g). Black curve in (d) shows two well separated pixels of the same view on the retina. (e-f) show the case when light from two lenslets forms different views (angles) but creating the same out-of-focus point, as shown in sketch (h).

Depth positions with more than 2 views entering the pupil

In this section we visualize the blurred images of different depth points, each of which is formed by two beams (rays) from the two lenslets, as described in the previous section. These two beams land on the retina to form two spots whose spacing determine whether they are perceived as in-focus or out-of-focus. Figure 5(a) shows normalized spacing between the two spots formed by Lens 1 and Lens 2 rays. The spacing is normalized by the sum of their half widths. Every point on the plot represents image of a depth point formed on the retina by intersection of two rays creating either in-focus or out-of-focus points. For any ID, these two rays analyzed will form only one of these in-focus or out-of-focus points, not all of them. Other lenslets and pixel combinations of the same ID will form other depth points at different lateral positions. But since the geometry of the rays remains the same, we just use a pair of rays to analyze most of depths. The depth points may be formed by intersection of two or more rays but the angular spacing of the intersecting rays remains the same. Therefore, the spacing between any two spots (retinal image of a single point) on the retina remains the same. Thus, we analyze only two rays. With this plot we can visualize all those possible points at once. For the ease of visualization and understanding, we plot normalized spacing as opposed to absolute spacing. This is because for each of the points in the plot we need to determine whether the two spots are well separated (resolved) or not. We have used the spacing between the spots to be greater than the sum of half-widths as the criterion for separation. In the normalized plot, the well separated spots are shown as value 1 or greater than 1 and the not resolved spots are shown as value between 0-1. Please note that even the two separated spots are

supposed to from a single depth point, but they seem to be separated on the retina because of low angular sampling. This makes these out-of-focus depth points to have a discontinuous (aliased) blurred image which is different from the smooth blurred image of a real world out-of-focus point.

The x-axis of these plots is the pixel position on the screen away from the center of lens 2. The pixel position on the screen is geometrically related to the emission angle from the lenslet. This emitted ray intersects with the on-axis ray from lens 2 to form the out-of-focus depth point. Please note that in the explanation and discussion of all the plots in the paper, we have interchangeable used the words 'pixels', 'views', and 'angles', which are all directly related to each other. For E.g. two ray angles intersecting means two views are intersecting, which also means rays from two pixels are intersecting.

To understand this plot, assume that the eye is focused at a fixed depth and the two rays form one of the out-of-focus points. The in-focus point is assumed to be formed by another lenslet and pixel combination and is shifted slightly laterally, but still landing on the fovea. The eye is viewing both the in-focus and out-of-focus points simultaneously on the fovea. This plot reveals the out-of-focus blurred spots which are not resolved (have a single smooth blurred spot) or are fully resolved (image seems to be formed by discrete spots) on the retina.

One few key observation from Fig. 5(a) that there is a narrow range of depths close to the in-focus depth for which there is a continuous blur on the retina. Other points far away from the focus position of the eye will have a blurred spot consisting of two distinct spots on the retina. Thus blurred spots for these depths will not seem continuous.

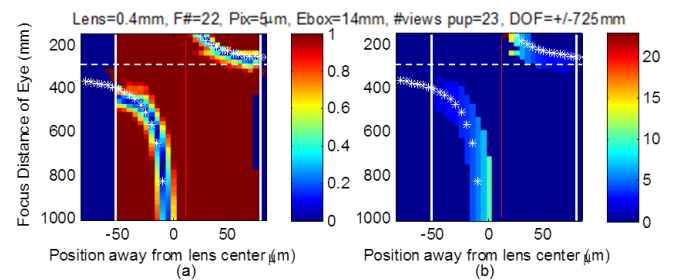


Figure 5: (a) Visualizing the quality of out-of-focus blurred spots formed on the retina. Each blurred spot is formed by two spots from the two rays landing on the retina. Normalized separation between the two spots from lens 1 and lens 2 on the retina is plotted. x-axis gives varying pixel position on the screen, away from the center of lens 2 (equivalent to emission angle from the lenslet) and y-axis gives the focus position of the eye when eye is located at a distance of zero. ID, marked with the horizontal white dashed line, is located at a viewing distance of 300 mm from the eye. White asterisks show geometrically calculated position of the depth object for the corresponding screen pixel position on the x-axis. Dark blue regions beyond the white vertical stripes show the pixel positions for which the ray from lens 2 misses the pupil. Total number of views (or angles or pixel locations) entering the pupil can also be noted from the number of horizontal points in the maroon region. Regions with values higher than the normalized intensity 1, in maroon, show a blurred spot consisting of two well resolved spots on the retina. Colored regions are where the blurred spot consists of two spots which are not well resolved, and hence contribute to a larger single smooth spot on the retina. Red vertical line shows the pixel location or the emission angle which intersects ray from lens 1 at the pupil and hence contributes as a different pixel of the same view on the retina; which is also the center of the elemental image for this lens. (b) Plot of number of views (or screen pixels) contributing to the formation of that spot for each depth position. Eye pupil size is 4 mm.

Figure 5(b) shows a plot of the number of views entering the pupil vs the object depth. For each pixel position of the screen on

the x-axis, we determine the lateral spacing between the two rays when they land on the pupil and determine how many such views can fit in the pupil to calculate the number of views entering the pupil. All these views come from the same depth point. Two key observations from this figure are – 1) there are depth positions very close to the ID, both in front and behind, for which only a single view enters the eye. This is due to large emission angle of the ray from the lenslet or far pixel position in the elemental image, which therefore misses the eye. For these depths, only a single view enters the pupil implying that the viewer can only perceive depth through stereopsis. 2) As seen, the depth points which are farther from the display (both in the front and behind) have more views entering the eye. As the object gets closer, fewer views enter the pupil. For depths very close to the display (the region beyond the vertical white stripes), only a single view enters the eye. This result has not been noted previously. But this has a drastic implication: the number of views entering the eye is a function of the object depth. This means that even though a large number of views may enter the pupil, for most depths, the number of views forming the depth point is much lesser. For E.g., for the ID in the Fig. 5, 23 views enter the pupil but only 5 or fewer views combine to form depth points between 250 mm-600 mm.

Varying screen pixel pitch

Next, we analyze the changes in the retinal image spots when the pixel pitch is varied. Figure 6 shows changes in various properties of the out-of-focus blurred spot – the separation of two contributing spots, number of views, and the blurred spot width - with varying pixel pitch. The first observation is an already known fact: that number of discrete depth points is reduced with fewer views or larger pixel pitch.

Our key observation, as explained below, is that the benefits of very large number of views in the ID is limited by the depth of field (DOF), the spatial resolution and the diffraction blur the eye. By considering all these we determine an optimal number of views in the eye's pupil that give good depth perception. Note that we report the cutoff in number of views for a given pupil size and not in pixel size of the screen. This is because the pixel size can be calculated from the number of views and other display parameters, namely, lens pitch, lens $f/\#$ and viewing distance.

The plots in the first column in Fig. 6 show normalized separation between the two spots, similar to Fig. 5(a). The details and description are the same as given in the previous section i.e. we visualize all the possible out-of-focus blurred spots simultaneously on the retina and note if they have continuous blurred spot or not. However, here we compare the same plot for varying pixel pitches of the ID.

From Fig. 6, the first observation we note is that the number of possible out-of-focus points with continuous blur reduce as fewer views enter the pupil. Continuous blur is defined by separation distance of the two contributing spots. When this separation is less than the width of the spots, then the eye cannot resolve whether it is a single continuous spot or two spots. The out-of-focus points with continuous blur can be seen by picking any focus position of the eye in the plots in column 1 and noting the number of points along that horizontal line with value < 1 . When comparing IDs with different pixel pitches and hence different number of views in the pupil, we note that for the ID with 120 views, there are many such out-of-focus points. For ID's with 23 and 12 views, there are at least 1-4 out-of-focus points. But for the ID with 6 views, only 0-2 possible out-of-focus points exist. So

for the ID with 6 views, there are certain eye focus positions for which no out-of-focus points with continuous blur exist. Thus, fewer views provide fewer out-of-focus points with continuous blur. The ID with 12 views will give at least one such point for every in-focus depth.

Next, we look at the DOF in the IDs and the real world. Figure 7 shows DOF of the eye in the real world for comparison. In Fig. 6, the ID pixel pitch is varied such that 120, 23, 12 and 6 views enter the eye. Comparing the IDs with 120 and 23 views against the DOF of the eye, we see that a very large number of depth points are unnecessary as they fall within the DOF of each other. The ID with 6 views has depth points spaced very far apart and thus falling out of the DOF of each other. This will not give a perception of continuous depth when viewing this ID. Therefore, with keeping the DOF of the eye in mind, approximately 12 views (the 3rd row plots) in a 4 mm pupil are optimal.

Third, we compare absolute separation between the two spots, in pixels of the eye, for different IDs. The pixel (cone) size of the fovea region in the retina is assumed to be $2.5 \mu\text{m}$. The plots are shown in the third column in Fig. 6. The negative and positive spacing values represent depth points lying in front or behind of the object in focus, respectively. In that column, plots in rows 2 and 3, the IDs with 23 and 12 views respectively, are very similar to row 1 (120 views) but plot in row 4 (6 views) is highly quantized and not an accurate representation of row 1. Therefore, due to limited pixel size of $2.5 \mu\text{m}$ at the fovea, a higher density of views than about 12 again is not needed.

Fourth, from comparing the blurred spot sizes in the 4th and 5th columns for the ID and the real world, respectively, we see that about 12 views seems to be a reasonable cutoff to have an accurate representation of the real world blur for out-of-focus points. The blur size refers to full spot size formed by overlapping of all the rays on the retina from that depth point; it is not the spot formed by just two views on the retina. As can be seen in the plot, more views are definitely better but are not needed. And fewer views give a very sparse representation of the true blur.

This is just one example of an ID with varying pixel sizes while keeping other parameters fixed. We did the simulation with different lens pitches and $f/\#$ s. Two different examples are shown in Fig. 8 and 9. We also did the simulations for 500mm viewing distances and 2-6 mm eye pupil sizes. In all the different cases we observe that roughly 10 views along one direction in a 4 mm pupil is the cutoff to start mimicking the real world conditions. Approximately, 10 views give enough depth points for the eye to focus and enough out-of-focus points with continuous blurred spots. We also observe that 20 views are more than sufficient to exactly recreate an ID matching the real world.

Discussion and Analysis

In the paper, we presented a new method to study Integral displays by doing light propagation simulation from the lenslet to the retina. This method has advantages over performing a ray-trace analysis as it accounts for effects of diffraction from various optical elements and their apertures. With this we are able to compute true spot sizes on the retina which is not accurately given by geometrical optics.

In this study of IDs we specifically focused on providing how accurately the in-focus and out-of-focus depth points are rendered on the retina. This study allowed us to understand the capability of these displays to mimic the real world behavior. However, our results have not been verified with visual perception studies. Currently available large displays don't offer pixel pitches small

enough to build an ID that provides the desired number of views reported by this study.

We only simulated and reported results for far-eye integral displays with the screen-lens spacing equal to the focal length. The same simulation method can also be extended to understand properties of other types of ID configurations, such as IDs with spacing shorter or longer than the focal length, which have been used for near-eye IDs or other light field displays.

Also note that the simulation and the results are for 1D. For 2D, if we assume all the optics and retinal sampling to be circularly symmetric, the results can be extended to be circularly symmetric or even square.

In our analysis, we have assumed that both the in-focus and out-of-focus objects are simultaneously visible to the viewer on the fovea. Therefore, we have used the resolution at the fovea to obtain the results presented here. It is reasonable to assume that the in-focus point will be on the fovea. However, the out-of-focus points can be easily located at the periphery. When the depth points are seen in the periphery of the eye, far fewer views than reported here would be needed as the eye resolution is low in that region. So, fewer views may render accurate blur for the periphery.

We also note that here we are only considering out-of-focus points formed by two adjacent lenslets. However, there are many additional depth points possible from other lenslets as shown in Fig. 2. For E.g., depth points formed by the intersection of other rays from lens 1 and lens 2 or the rays from lens 1 and lens 3 or the rays from lens 1 and lens 4 and so on. When considering all these possible cases, the total number of in-focus and out-of-focus depth planes can be much more than mentioned here. If we consider these depth points as well, then fewer views than 10 can provide enough depth planes to satisfy the DOF and enough blurred depth planes criteria mentioned above. However, the criterion of matching the real world blurred spot size still requires at least 10 views.

Finally, even though we have presented results here for a fixed eye pupil width, we did simulations for eye pupil varying from 2-6 mm. We found that the results match what is presented here. The result of 10 views for 4 mm pupil can be translated as 0.4 mm view spacing and scaled for a different pupil size, for E.g., 5 views for 2 mm eye pupil. Thus we note that the results in this paper can also be interpreted as optimal view spacing for simulating accurate blur.

Summary of Results

The key results presented in this paper have not been shown previously for far-eye IDs. We think that these results will be very useful in designing IDs which are already constrained by limited pixel sizes and trade-offs in the characteristics.

In a far-eye ID, when the spacing is equal to the focal length, the number of discrete depth positions which can render blur is fewer than total depth points. This means that only few of these discrete depths have 2 or more views (ray angles) entering the pupil. Other depth planes rendered by the ID can only deliver a single view to the eye implying that those depths can only give depth perception from stereo.

The other observation is that each depth plane has a different number of views contributing to its blurred spot formation. This number is not the same for all the depth points, but depends on the total number of views entering the eye. The depth points close to the ID, both in the front and behind, have fewer views contributing to it than the total number of views entering the eye's pupil. Also, this number stays the same for a given depth even when the

number of views in the pupil is increased by reducing the pixel size (keeping other parameters the same).

The final result we have shown is that roughly 10 views are needed in a 4 mm sized eye pupil to reasonably approximate the real world viewing conditions of supporting enough blurred depth planes and retinal blur. In other words, this can be understood as ~0.4 mm view spacing on the pupil to be optimal. We also observed that 20 views are more than sufficient to exactly recreate an ID matching the real world. In derivation of this result we have taken into account the DOF of the eye, the spatial resolution of the fovea and diffraction blur of the eye. We also note that as previously shown, 2-3 views in the pupil may start triggering accommodation response, but a much higher density of views is needed to mimic the real world blur.

References

- [1] G. Lippmann, "Épreuves réversibles donnant la sensation du relief," *Jour. of Phy.*, vol. 7, no. 4, pp. 821–825, 1908.
- [2] J. Geng, "Three-dimensional Display Technologies," *Adv. Opt. Photon.*, vol.5, no. 4, pp. 456-535, 2013.
- [3] D. Lanman, D. Luebke, "Near-Eye Light Field Displays," *ACM Trans. Graph.*, vol. 32, no. 6, article 220, 2013.
- [4] H. Hua and B. Javidi, "A 3D Integral Imaging Optical See-through Head-mounted Display," *Opt. Express*, vol. 22, no. 11, pp. 13484-13491, 2014.
- [5] S. Park, J. Yeom, Y. Jeong, N. Chen, J. Hong and B. Lee, "Recent Issues on Integral Imaging and its Applications," *Jour. of Info. Disp.*, vol. 15, no. 1, pp. 37-46, 2014.
- [6] J. Burge, R. Held, and M. S. Banks, "Blur and Accommodation are Metric Depth Cues," *Jour. of Vision*, vol. 8, no. 6, pp. 80, 2008.
- [7] Y. Takaki, "High-Density Directional Display for Generating Natural Three-Dimensional Images," *Proc. IEEE*, vol. 94, no. 3, pp. 654-663, 2006.
- [8] H. Huang and H. Hua, "Systematic characterization and optimization of 3D light field displays," *Opt. Express* vol. 25, no. 16, pp.18508-18525, 2017.
- [9] S. Min, J. Kim and B. Lee, "New Characteristic Equation of Three-Dimensional Integral Imaging System and its Applications," *Jap. Jour. of App. Phys.*, vol. 44, no. 2, pp. L71–L74, 2005.
- [10] B. E. A. Saleh and M. C. Teich, *Fundamentals of Photonics*, Second Edition, Chap. 4, Wiley-Interscience, 2007.
- [11] J. W. Goodman, *Introduction to Fourier Optics*, Third Edition, Eqn. 5-25 and 5-26, Roberts & Company, 2007.
- [12] R. T. Held, E. A. Cooper and M. S. Banks, "Blur and Disparity Are Complementary Cues to Depth," *Current Biology*, vol. 22, no. 5, pp. 1-6, 2012.

Author Biography

Ginni Grover is a senior research scientist at the Computational Imaging Lab in Intel Labs. She received her B. Tech. from IIT Delhi and her Ph.D. from University of Colorado at Boulder. Prior to joining Intel she worked at Double Helix LLC, a startup for 3D microscopy. Her work has focused on optical design, simulation and development of different methods of 3D imaging and displays such as multi-camera arrays, light field capture and 3D displays.

Oscar Nestares is a Principal Engineer at Intel Labs working on computational imaging algorithms, lightfield processing, and video enhancement. Before he was a tenured Research Scientist (Institute of Optics, CSIC) working on visual system models and biologically inspired image and video processing and analysis, a Fulbright Scholar at Stanford University, and a consultant at Xerox PARC. He received his M.S. (1994) and Ph.D. (1997) in Telecommunication Engineering from Universidad Politécnica de Madrid.

Ronald Azuma received a B.S. in EECS from UC Berkeley and an M.S. and Ph.D. in Computer Science from UNC Chapel Hill. He previously worked at HRL Laboratories and Nokia Research Center. He is currently a Principal Engineer and Research Manager in Intel Labs. His background includes Augmented and Virtual Reality, tracking systems, and computational displays. He became an IEEE Fellow in 2016.

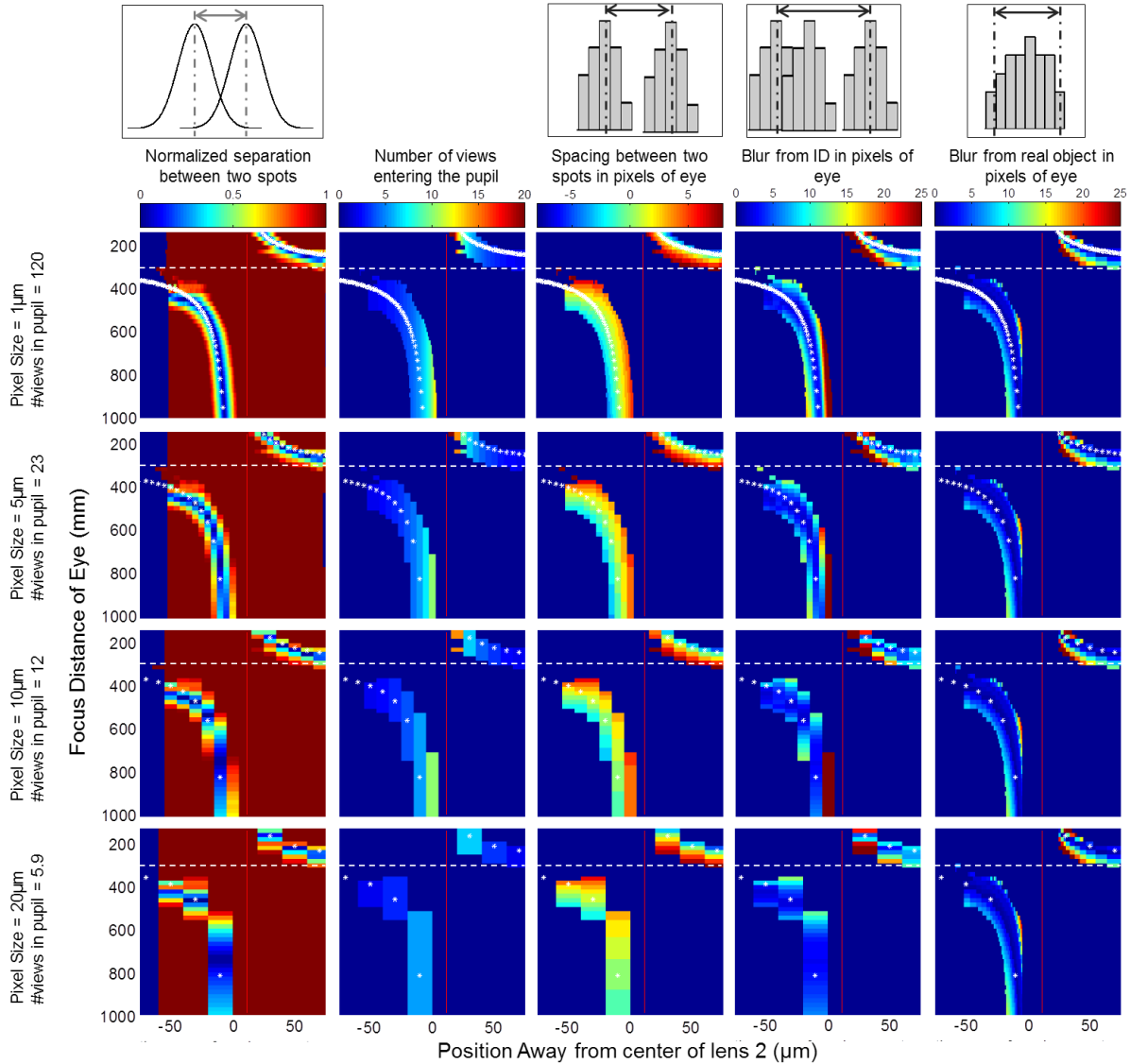


Figure 6: Plots for an Integral Display with 0.4 mm lens pitch, $f/\#$ 22 and 14 mm eyebox at 300 mm view distance. ID, marked with the horizontal white dashed line, is located at a viewing distance of 300 mm from the eye. Eye pupil size is 4 mm. Pixel size of the fovea is assumed to be $2.5 \mu\text{m}$ for the plots in the last three columns. Each row represents a different pixel pitch of the screen ($1 \mu\text{m}$ pixels providing 120 views, $5 \mu\text{m}$ pixels providing 23 views, $10 \mu\text{m}$ pixels providing 12 views, & $20 \mu\text{m}$ pixels providing 5.9 views). Each column represents a different plot as described schematically and in words on the top. Colorbar for each plot is also given at the top. White curve with asterisks represents geometrically calculated depth position for that pixel position. Red vertical line in each plot represents the pixel position when the ray from lens 2 intersects the ray from lens 1 at the pupil. Since column 5 depicts the blur from real objects, the image is of course the same in each row and is replicated to provide side-by-side comparisons with column 4.

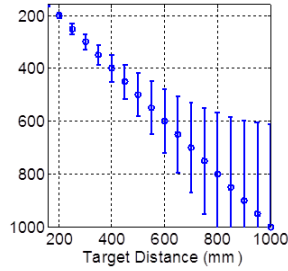


Figure 7: Plot showing depth-of-field of the human eye for different depth positions. Adapted from disparity to blur equation in Ref. [12]

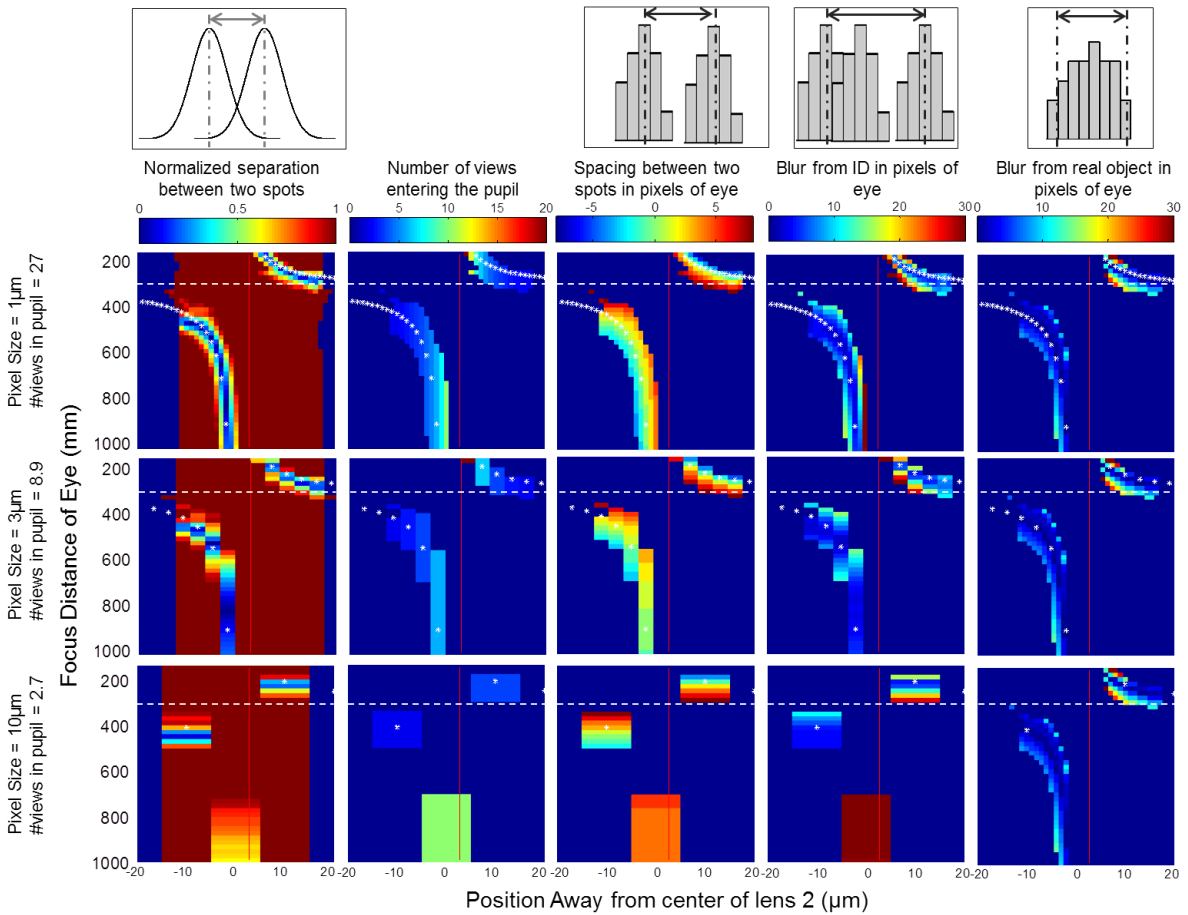


Figure 8: Plots for an Integral Display with 0.4 mm lens pitch, $f/\#5$ and 60 mm eyebox at 300 mm view distance. ID, marked with the horizontal white dashed line, is located at a viewing distance of 300 mm from the eye. Eye pupil size is 4 mm. Pixel size of the fovea is assumed to be $2.5 \mu\text{m}$ for the plots in the last three columns. Each row represents a different pixel pitch of the screen ($1 \mu\text{m}$ pixels providing 27 views, $3 \mu\text{m}$ pixels providing 8.9 views, & $10 \mu\text{m}$ pixels providing 2.7 views). Each column represents a different plot as described schematically and in words on the top. Colorbar for each plot is also given at the top. White curve with asterisks represents geometrically calculated depth position for that pixel position. Red vertical line in each plot represents the pixel position when the ray from lens 2 intersects the ray from lens 1 at the pupil. Since column 5 depicts the blur from real objects, the image is of course the same in each row and is replicated to provide side-by-side comparisons with column 4.

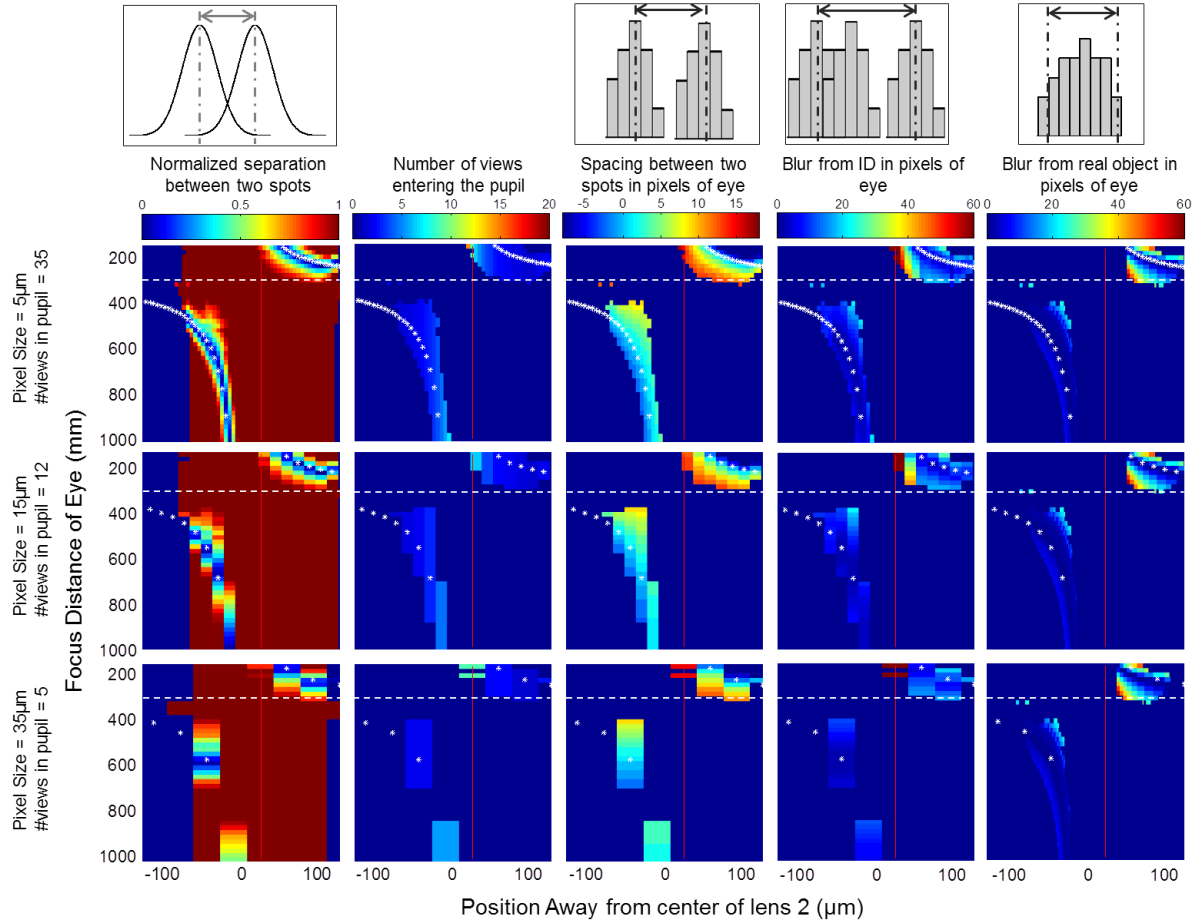


Figure 9: Plots for an Integral Display with 0.6 mm lens pitch, $f\#22$ and eyebox 14 mm at 300 mm view distance. ID, marked with the horizontal white dashed line, is located at a viewing distance of 300 mm from the eye. Eye pupil size is 4 mm. Pixel size of the fovea is assumed to be $2.5 \mu\text{m}$ for the plots in the last three columns. Each row represents a different pixel pitch of the screen ($5 \mu\text{m}$ pixels providing 35 views, $15 \mu\text{m}$ pixels providing 12 views, & $35 \mu\text{m}$ pixels providing 5 views). Each column represents a different plot as described schematically and in words on the top. Colorbar for each plot is also given at the top. White curve with asterisk represents geometrically calculated depth position for that pixel position. Red vertical line in each plot represents the pixel position when the ray from lens 2 intersects the ray from lens 1 at the pupil. Since column 5 depicts the blur from real objects, the image is of course the same in each row and is replicated to provide side-by-side comparisons with column 4.

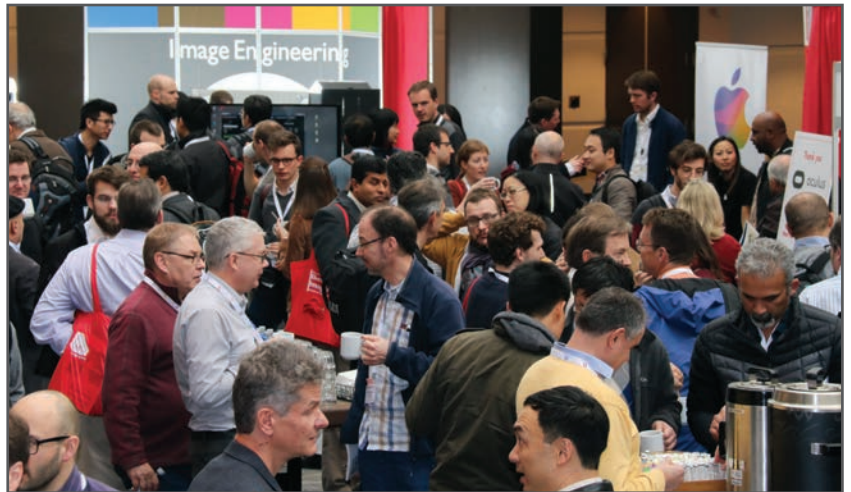
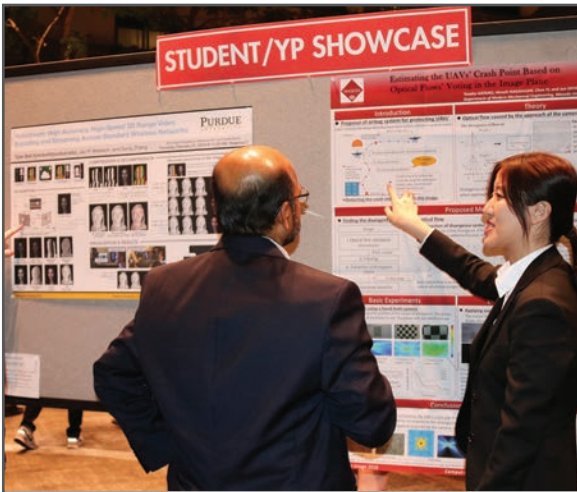
JOIN US AT THE NEXT EI!

IS&T International Symposium on

Electronic Imaging

SCIENCE AND TECHNOLOGY

Imaging across applications . . . Where industry and academia meet!



- **SHORT COURSES • EXHIBITS • DEMONSTRATION SESSION • PLENARY TALKS •**
- **INTERACTIVE PAPER SESSION • SPECIAL EVENTS • TECHNICAL SESSIONS •**

www.electronicimaging.org

